

Comparison of the reactivity of bulk and surface oxides on Pd(100)

Y. Yun^a, J. Wang^b, E.I. Altman^{a,*}

^a Department of Chemical Engineering, Yale University, New Haven, CT 06520, USA

^b Department of Physics, Yale University, New Haven, CT 06520, USA

Received 18 September 2007; revised 30 October 2007; accepted 31 October 2007

Abstract

The reactivity of bulk PdO clusters produced by plasma oxidation of Pd(100) towards propene oxidation was characterized using temperature programmed desorption (TPD) and isothermal oxygen titration. The TPD results were dominated by simultaneous CO₂ and water desorption in a peak at 490 K. The only other product observed was a small amount of CO near saturation propene coverages that also desorbed at 490 K. The propene coverage saturated at exposures between 0.5–1 l, indicating a sticking coefficient close to one. In the titration experiments, CO₂ production peaked almost immediately upon exposure to propene, indicating that the propene oxidation rate fell as the surface was reduced. Above 450 K, virtually all of the propene was completely oxidized to CO₂ and water, while at lower temperatures small amounts of CO were observed and unreacted propene fragments accumulated on the surface. In comparison, previous results for a well-ordered surface oxide on Pd(100) were similar in that CO₂ and water also desorbed simultaneously indicating a similar mechanism, but different in that the sticking coefficient on the surface oxide was a factor of 20 lower, and the desorption peaked 60 K lower. These differences cause the bulk oxide to be far more active at higher temperatures than the surface oxide, but the surface oxide displays some activity down to lower temperatures where propene simply accumulates on the bulk oxide surface.

© 2007 Elsevier Inc. All rights reserved.

Keywords: Palladium; Palladium oxide; Propene; Oxidation; Temperature programmed desorption; Titration

1. Introduction

Although transition metals have generally been considered more reactive than their corresponding oxides, over the last few years it has been suggested that under certain conditions the oxides may be far more active catalysts. The most extensively studied example has been CO oxidation over Ru where it has been suggested that RuO₂ may be more active than Ru at low temperatures [1–4]. A recent study, however, showed that under stoichiometric conditions the active surface is 1 ml of O in a state better described as a surface oxide [5]. Palladium oxidation catalysis has attracted considerable attention in recent years because of practical interest in exploiting its high activity for total hydrocarbon oxidation, and because of lingering fundamental questions about whether bulk Pd oxide or adsorbed oxygen phases on metallic Pd are responsible for the high ac-

tivity. While low pressure surface science studies have shown that increasing the oxygen coverage on Pd inhibits the adsorption of CO and hydrocarbons leading to low reactivities [6–9], kinetic studies performed at higher pressures have suggested that PdO is more active than Pd, at least at lower temperatures [10,11]. A possible reason for this discrepancy is that it has been difficult to form bulk PdO by exposing Pd single crystals to molecular oxidants in UHV. Therefore, we have been using an oxygen plasma to increase the oxygen coverage by 1–2 orders of magnitude above that achievable by dosing O₂ or NO₂ [12–14]. In this paper, it will be shown that the sticking coefficient for propene on the bulk PdO formed by plasma oxidation is close to one, allowing it to be highly active under conditions where the surface oxide formed by exposure to molecular oxidants is unreactive towards propene.

Palladium oxidation is a complex process that involves a number of surface phase transitions before bulk oxidation occurs [13,15,16]. For Pd(100), initial exposure to oxygen results in chemisorption atop the surface in p(2 × 2) and c(2 × 2) structures. Once the c(2 × 2) structure saturates, oxygen moves

* Corresponding author.

E-mail address: eric.altman@yale.edu (E.I. Altman).

below the surface ejecting Pd atoms onto the surface that either form islands or attach to pre-existing steps; the surface periodicity does not change in this stage. After island growth stops, the surface reconstructs to form (5×5) or $(\sqrt{5} \times \sqrt{5})R27^0$ structures, depending on the temperature. The higher temperature $(\sqrt{5} \times \sqrt{5})R27^0$ structure has been attributed to a ruffled PdO(101) monolayer [17]; throughout the remainder of this paper this phase will be referred to as a surface oxide. Under UHV conditions it has been difficult to increase the oxygen coverage much beyond this surface oxide; however, exposure to either ambient pressure O₂ or an oxygen plasma leads to three-dimensional PdO clusters on the surface [11,14,18,19].

We previously characterized the effect of oxygen coverage on propene oxidation on Pd(100) up to saturation of the surface oxide [7]. In temperature programmed desorption (TPD) experiments of propene on the $(\sqrt{5} \times \sqrt{5})R27^0$ reconstructed Pd(100) surface, CO₂ and water were produced simultaneously at 430 K. In contrast, on the $p(2 \times 2)$ and $c(2 \times 2)$ chemisorbed oxygen phases on Pd(100), propene dissociated to form water at 430 K while almost all the CO₂ was formed by oxidation of surface C at 550 K. These results showed that propene oxidation favors a more facile pathway at high oxygen coverages. The initial propene sticking coefficient, however, was found to be a factor of five lower on the $(\sqrt{5} \times \sqrt{5})R27^0$ surface than on the (2×2) phases. Isothermal oxygen titration experiments at 500 K showed that propene oxidation is slowest at the highest oxygen coverages and maximizes just before all the oxygen is removed from the surface. These results indicated that oxidizing the Pd surface affects propene oxidation in two contradictory ways: it decreases the propene adsorption probability, but favors a low activation energy pathway once the molecules adsorb. Similar measurements for CO also indicated that the surface oxide is relatively unreactive compared to chemisorbed oxygen phases because of the inability of the surface oxide strongly adsorb the CO [20–22].

We recently showed that oxygen coverages on Pd(100) could be increased by almost two orders of magnitude in UHV by exposing the surface to oxygen atoms generated by a microwave plasma [14]. The additional oxygen is incorporated into the surface in the form of poorly ordered bulk PdO clusters on the surface. The oxide clusters decomposed at essentially the same temperature as the surface oxide. Further, low energy ion scattering indicated that the surface oxide and the oxide clusters exposed similar densities of Pd sites on the surface. In this paper, the reactivity of the PdO clusters towards propene oxidation will be described. It will be shown that unlike the surface oxide, the propene sticking coefficient on the oxide clusters is close to one, while the reaction mechanism on the oxide clusters is similar to that on the surface oxide where CO₂ and water form simultaneously. Although the activation energy for the reaction step was higher on the oxide clusters, the higher sticking coefficient made the bulk oxide more active at temperatures above ~450 K. Meanwhile, surface C formed by hydrocarbon dissociation on the chemisorbed oxygen-covered metal surface does not desorb until 550 K, making the oxide clusters more reactive than metallic Pd at least up to that temperature.

2. Experimental

The experimental procedures and facilities have been described in detail previously [14]. Briefly, experiments were performed using a UHV system equipped with the necessary sources and analyzers for temperature programmed desorption (TPD), Auger electron spectroscopy (AES), X-ray photoelectron spectroscopy (XPS), ion scattering spectroscopy (ISS), low energy electron diffraction (LEED), and scanning tunneling microscopy. Reactive oxygen species were generated using a differentially pumped Tectra Gen II microwave electron cyclotron resonance plasma source. Under typical operating conditions, the source is estimated to generate an atomic oxygen flux of $2.4 \times 10^{13} \text{ cm}^{-2} \text{ s}^{-1}$. For most of the experiments described in this paper, the Pd(100) surface was exposed to the plasma source for 10 min at 550 K, which was previously shown to produce an oxygen coverage of 10.8 ml, or alternatively a nominal oxide thickness of 3.4 nm [14]. Mounting and preparation of the Pd crystal has been described previously [12].

Polymer grade propene C₃H₆ (Airgas Specialty Gases) with a minimum purity of 99.5% was used in the experiments. The major impurity in the gas was specified as propane at a typical level of 4000 ppm. Alkanes do not react with oxygen-covered Pd under the conditions employed in this study so this impurity does not affect the results [23]. Because the C₂H₄ fragment from C₃H₆ has essentially the same mass as CO in the mass spectrometer traces, C₃D₆ was also used in some experiments to distinguish combustion products from possible partial oxidation products. No differences were observed for the CO (mass 28) and CO₂ product traces after C₃H₆ and C₃D₆ dosing in TPD and oxygen titration experiments, indicating that ethene can be excluded as a reaction product. Although the system was fitted with a capillary array doser, propene was dosed with the sample turned away from the doser so that doses are calculated by simply multiplying the increase in background pressure by the exposure time.

To distinguish CO produced by propene oxidation from CO produced by CO₂ cracking in the mass spectrometer, CO₂ was leaked into the chamber to determine the CO:CO₂ cracking ratio for the mass spectrometer in our experimental configuration. A value of 0.16 was obtained. The contribution of CO₂ cracking to the CO signal was subtracted in all of the data shown in this paper by multiplying the CO₂ trace by this factor. The relative mass spectrometer sensitivity to CO₂ and CO was determined by leaking the gases into the chamber and measuring the increase in the mass spectrometer signal for a given rise in background pressure as measured by an ion gauge. It was found that the system was 1.9 times more sensitive to CO than CO₂.

Isothermal oxygen titration measurements were used to calibrate the coverages in the TPD experiments. In these measurements, the surface was exposed to NO₂ at 550 K which results in a saturation coverage of 0.9 ml of oxygen [7]; subsequent exposure to CO above 400 K removes all of the oxygen as CO₂ [21]. Integrating the rise in the CO₂ mass spectrometer signal during the CO exposure then provides a known standard to which the CO₂ peak integrals following propene exposure could be compared.

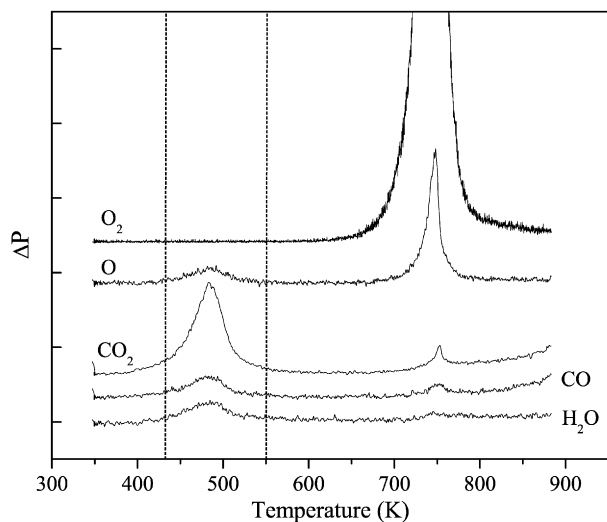


Fig. 1. Temperature programmed desorption traces for O_2 , O, CO_2 , CO, and H_2O obtained after exposing the plasma-oxidized Pd(100) surface to 0.25 L propene. The dashed lines highlight the position of the CO_2 desorption peaks for propene oxidation on a surface oxides on Pd(100) at 430 K and on chemisorbed oxygen-covered Pd(100) at 550 K. The data were offset so that each trace could easily be seen.

3. Results

The reactivity of the bulk PdO clusters was first characterized using TPD. Fig. 1 shows the desorption traces for CO_2 (44 amu), CO (28 amu), H_2O (18 amu), O_2 (32 amu), and O (16 amu) for a 0.25 L propene dose; other species corresponding to unreacted propene and potential partial oxidation products were monitored in initial runs, but no evidence of species other than combustion products were observed. Because of the large amount of oxygen on the surface, the O_2 signal is off-scale; however, the oxygen atom signal faithfully tracks the O_2 signal producing a sharp peak at the same position seen during O_2 TPD experiments. The small peak in the O signal at ~ 500 K is due to cracking of water, CO_2 , and CO. The strength of the oxygen signal indicates that the oxide remained largely intact after the 0.25 L propene dose. The figure also shows that CO_2 and water desorb simultaneously in a peak at 490 K, while very little CO was seen for this propene dose (the small CO_2 and CO peaks at 740 K are attributed to oxidation of C near the mass spectrometer filament; a small increase in these signals was seen whenever oxygen was leaked into the chamber). For comparison, the dashed lines in the figure indicate the temperatures at which CO_2 was observed after propene was exposed to the surface oxide and to (2×2) chemisorbed oxygen phases on Pd(100) [7]. While CO_2 forms on the bulk oxide at temperatures intermediate between the surface oxide and chemisorbed oxygen, the water evolves simultaneously with the CO_2 which is similar to the surface oxide but different from the chemisorbed oxygen phases where water is first observed followed by CO_2 at much higher temperatures. At these temperatures, H and O on Pd surfaces rapidly combine to form water which promptly desorbs from the surface [24]. Therefore, the simultaneous evolution of CO_2 and water from the surface oxide was attributed to a direct oxidation mechanism in which

rupture of the C–H bonds and oxidation of the carbon backbone follow in quick succession, as opposed to lower oxygen coverages on the metal surface where the molecules dissociate and then the fragments oxidize [7]. The results indicate that propene oxidation also follows a direct oxidation pathway on the bulk oxide clusters but with a higher activation energy than on the surface oxide.

Fig. 2 shows how the desorption traces evolve as the propene dose is varied. The figure shows single CO_2 and H_2O peaks at 490 K that do not appreciably change other than an increase in intensity as the propene dose is increased. The main oxygen desorption feature at 740 K is largely unaffected by propene exposure, while the weaker lower temperature feature associated with CO_2 , CO, and water desorption increases as the propene exposure increases. The most significant change in the traces as the propene exposure increases is the increase in CO production, from barely detectable below 0.25 L to almost 1/4 as intense as the CO_2 peak at 1 L. Taking into account differences in the mass spectrometer sensitivity to the two species, integrating the desorption curves indicates that the fraction of the carbon ending up as CO increases from below the detection limit at 0.1 to 0.13 at 1 L. The exposure dependence shown in Fig. 2 is considerably simpler than that previously seen for the surface oxide [7]. For the surface oxide, increasing the propene exposure first led to the appearance of a second CO_2 peak at 550 K, followed by an increase in the amount of CO produced, followed finally by the disappearance of the 550 K peak and accumulation of C on the surface. The appearance of the 550 K peak was due to a reduction of the surface oxide creating metallic regions of the surface where propene could dissociate, while the shift to CO production, the disappearance of the 550 K peak and the accumulation of C on the surface could all be attributed to insufficient oxygen on the surface to oxidize all of the adsorbed propene. In contrast, for the bulk oxide particles sufficient oxygen remains to prevent a transition to a metallic phase and so the only change that occurs is an increase in CO production that can be related to oxygen depletion from the outermost layer of the oxide.

Integrating the CO_2 and CO curves in Fig. 2 yields the uptake curves in Fig. 3. The curves show that the propene coverage saturates between 0.5 and 1.0 L indicating that the sticking coefficient was close to one. In sharp contrast, on the surface oxide, desorption signals were barely detectable after a 1 L dose and comparison of the uptake data suggests an initial propene sticking coefficient a factor of 20 lower on the surface oxide [7]. Combining the CO and CO_2 produced indicates that the propene coverage saturates at ~ 0.07 ML where a monolayer is defined in this case as number of molecules per number of Pd atoms on the original Pd(100) surface.

Propene oxidation kinetics were also characterized using isothermal oxygen titration experiments. In these experiments, the sample was oxidized by the plasma and then suddenly exposed to a constant propene pressure while potential reaction products were monitored with the mass spectrometer as a function of time. Similar to TPD, the rise in the partial pressure of the reaction products is proportional to their production rate and the integral of the curves to the total amount of product

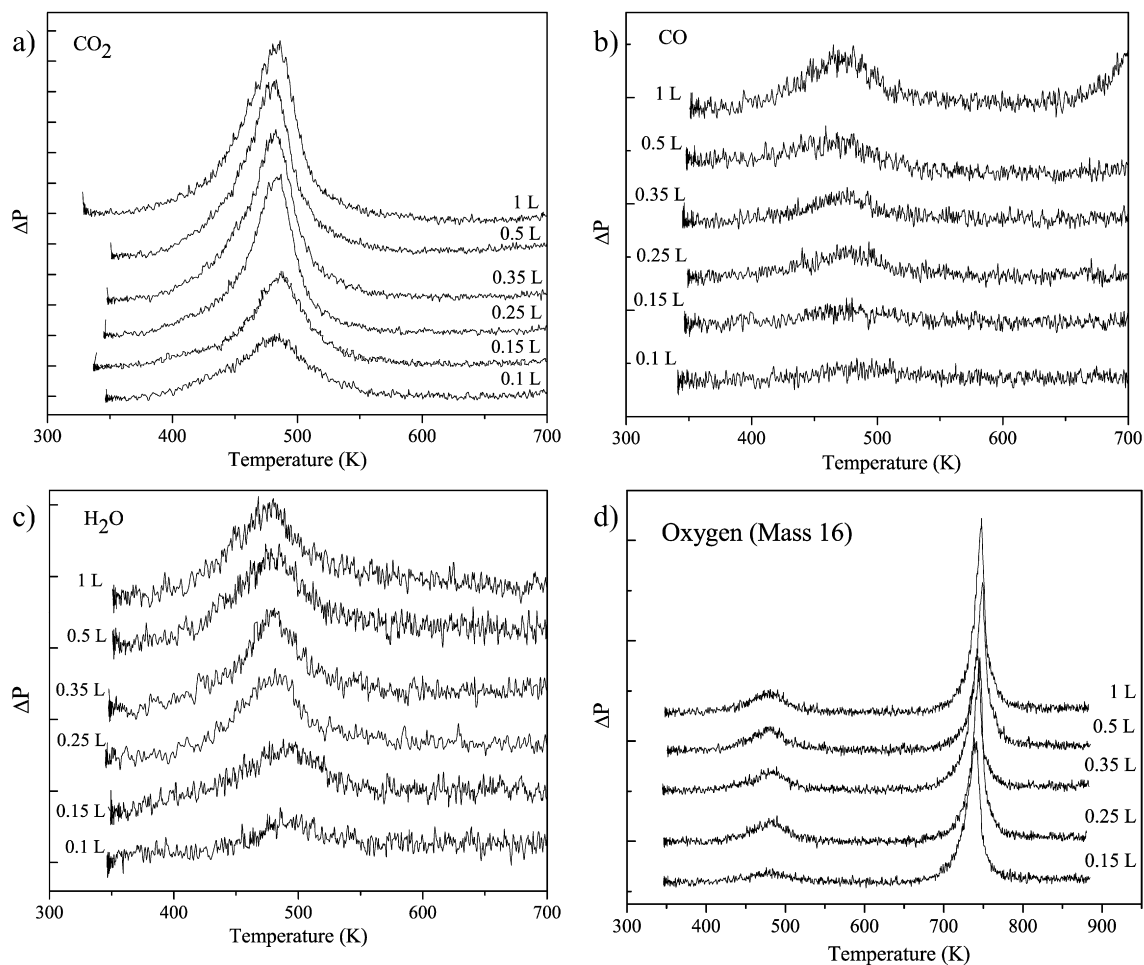


Fig. 2. Temperature programmed desorption results for a series of propene exposures to plasma-oxidized Pd(100). (a) CO₂, (b) CO, (c) H₂O, and (d) atomic oxygen. The data for each exposure were obtained simultaneously. The background was similar for each run, the data were offset for clarity.

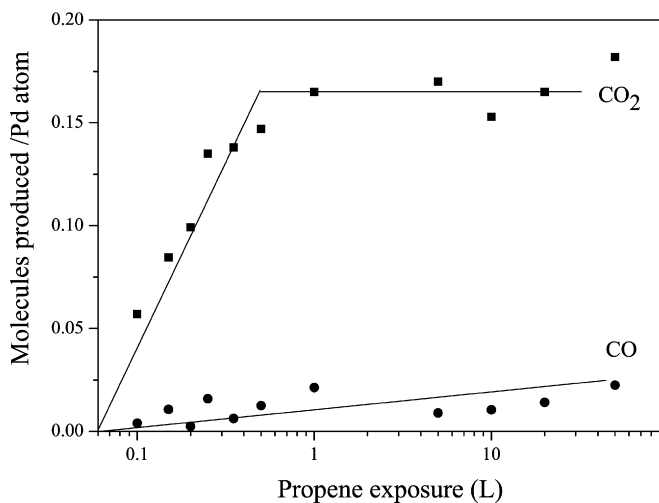


Fig. 3. Propene uptake curve for plasma-oxidized Pd(100) plotted as amounts of CO₂ and CO produced in TPD experiments versus the propene exposure. The data is corrected for differences in the mass spectrometer sensitivity to the two species and the CO₂ cracking contribution to the CO mass spectrometer signal.

produced [21]. Fig. 4 shows the CO, CO₂ and H₂O mass spectrometer traces for a Pd(100) surface oxidized for 10 min by the

plasma and then reduced by exposure to 6×10^{-8} Torr propene at 500 K. In addition to CO, CO₂ and H₂O, *m/e* ratios corresponding to cracking fragments for other potential oxidation products such as acetone and propanol were also monitored, but these showed no increase above background. The CO production from CO₂ cracking was subtracted in the same way as for the TPD data. The CO trace shows an initial jump up at the beginning and a jump down at the end corresponding to the times when the leak valve was opened and closed. Such jumps were observed whenever propene was leaked into the chamber and can be associated with propene cracking to C₂H₄⁺ in the mass spectrometer. On the other hand, the much larger initial jump in the CO₂ curve can be attributed to propene combustion. Fig. 4 shows that the CO₂ production rate maximized essentially immediately after the propene was leaked into the chamber; the rate then slowly decayed to zero. Meanwhile, the CO curve shows a much smaller decay after propene was leaked into the chamber, indicating that CO₂ was by far the predominant carbon containing oxidation product but that a small amount of CO was also produced. The ratio of the CO to CO₂ signal never significantly changed indicating that at 500 K, reduction does not alter the product distribution. Using estimates of the mass spectrometer sensitivities to CO and CO₂ suggests almost 15 times

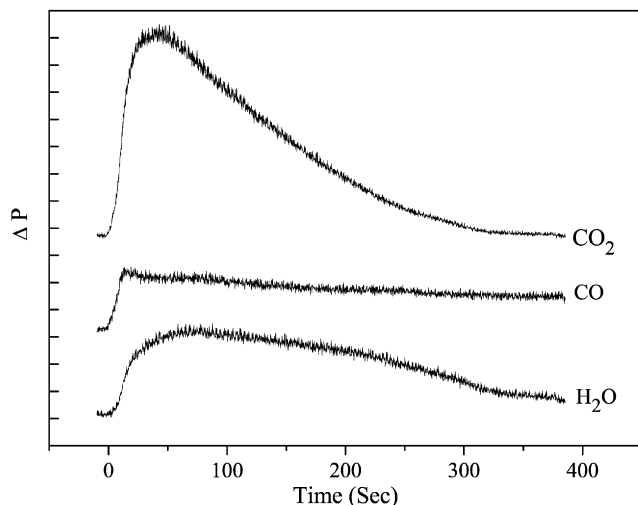


Fig. 4. Isothermal oxygen titration curves showing the rise in CO_2 , CO, and H_2O partial pressures when 6×10^{-8} Torr of propene was suddenly exposed to the plasma-oxidized Pd(100) surface at 500 K at $t = 0$ s. Most of the initial rise in the CO partial pressure is due to propene cracking in the mass spectrometer causing a rise in the signal at 28 amu. The traces have been offset for clarity.

as much CO_2 was produced as CO. In contrast to the CO_2 curve, water production did not maximize right after opening the leak valve. Instead, the H_2O trace reached a maximum 30 s later than the CO trace, and then slowly returned to the baseline.

Fig. 5 illustrates how temperature affects PdO reduction by propene. Fig. 5a shows that over the temperature range studied, CO_2 production always maximized almost immediately after propene exposure began, indicating that propene oxidation was fastest at the beginning of the reaction; i.e., when the surface was most oxidized. This reinforces the conclusion from the TPD results that showed a near unity initial sticking coefficient for the plasma oxidized surface, in sharp contrast to the surface oxide where the sticking coefficient increased after a slow initial reduction [7]. The CO_2 peak height, or maximum rate, increased as the temperature increased indicating that the reaction rate increases with increasing temperature. This also differs dramatically from the surface oxide where the maximum CO and propene oxidation rates decreased with increasing temperature, consistent with reactions limited by weak adsorption of the reactants [7,21]. At 500 K and above, the CO_2 curves almost linearly decayed back to the baseline, while at 450 K a second hump in the CO_2 curve could be seen, and at the lowest temperatures the curves show small peaks just after the leak valve was opened. The integrals of the curves are proportional to the total amount of CO_2 , and so comparing the curves it becomes obvious that as the temperature was decreased, the amount of oxygen removed through complete combustion of propene decreased; this is not surprising since the peak temperature in the TPD experiments was 490 K.

The CO traces in Fig. 5b indicate that the total amount of CO produced went through a maximum at 450 K. The CO curve for 450 K shows a peak that coincides with the hump seen in the CO_2 curve at the same temperature. Taking into account the mass spectrometer sensitivities, at the CO peak, the data suggest that the ratio of the CO to CO_2 production rates was

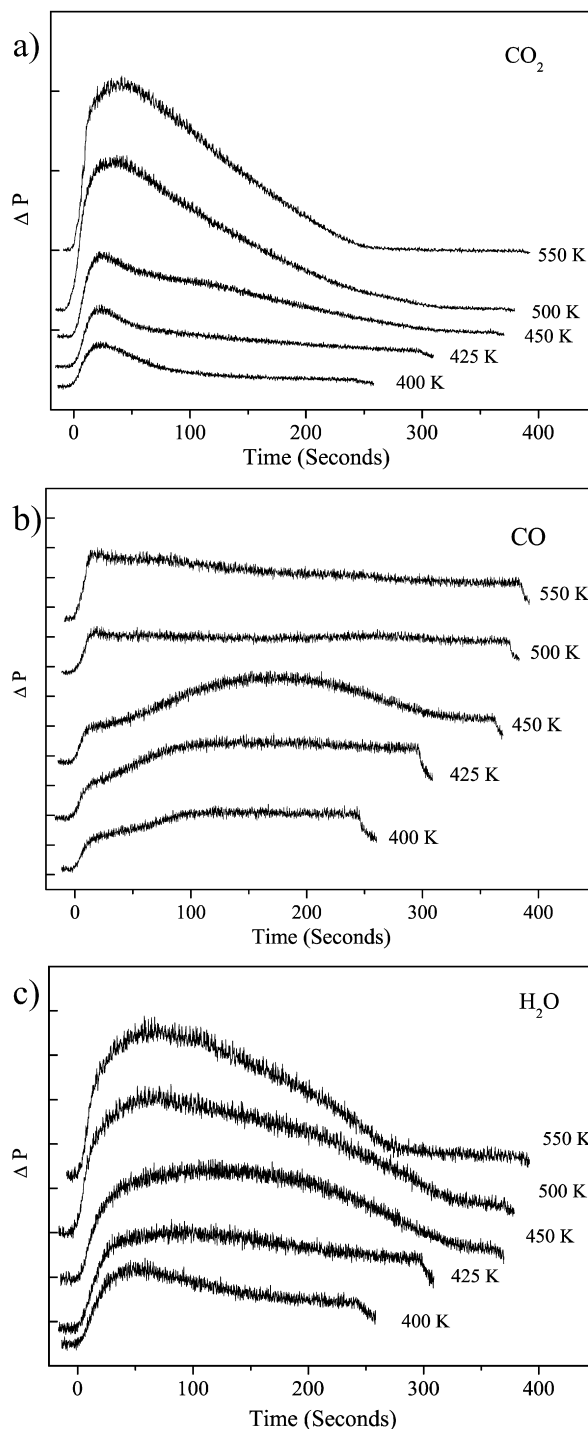


Fig. 5. Isothermal oxygen titration curves recorded at temperatures between 400–550 K. In each case, the surface was suddenly exposed to 6×10^{-8} Torr propene at $t = 0$ s while monitoring the rise in partial pressure of (a) CO_2 , (b) CO, and (c) H_2O . The background partial pressures were similar in each run; the curves were offset for clarity.

almost 0.5 compared to 0.03 immediately after the leak valve was opened. The increase in CO production after initial reduction at 450 K suggests that as the temperature is reduced below 500 K, limitations in the oxygen diffusion rate to the surface leave insufficient amounts of oxygen on the surface for complete combustion. At 400 and 425 K much smaller bumps in the

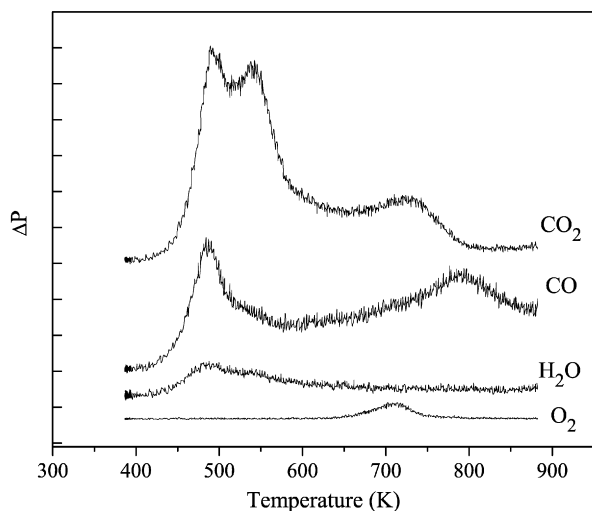


Fig. 6. Temperature programmed desorption data recorded following the oxygen titration experiment performed at 425 K pictured in Fig. 5. The total propene exposure was 18 L.

CO production rates were observed that can be attributed to the temperature moving well below the 490 K TPD peak temperature. As a result, propene and propene-containing fragments accumulated on the surface, as confirmed by TPD experiments performed after propene exposures that will be described below.

The water traces in Fig. 5c all show longer tails than the corresponding CO₂ traces. This may be due to two effects: (1) slow pumping rate for water compared to CO and CO₂ due to stronger adsorption of water on the walls of the vacuum chamber; and (2) strong adsorption of water on PdO. Although water does not strongly adsorb on metallic Pd or metallic Pd with lower oxygen coverages [25], water is considered to adsorb strongly on PdO [10,26]. This would suggest, however, that water should desorb at higher temperatures than CO₂ or CO in the TPD experiments, which was not observed.

Temperature programmed desorption experiments were performed following the lower temperature titration experiments to characterize the species remaining on the surface; curves obtained after reaction of the plasma-oxidized surface with propene at 425 K are shown in Fig. 6. In contrast to room temperature propene dosing, oxygen containing products were observed in several different peaks. The lowest temperature peaks for water, CO and CO₂ are seen at 490 K, the same as room temperature propene exposure except with a much larger CO to CO₂ ratio. These peaks can be associated with oxidation of nearly intact propene molecules, with the increase in CO production due to a lower surface oxygen concentration as described above. A second CO₂ peak accompanied by a shoulder in the CO trace occurred at 540 K, in the temperature regime where C atoms on Pd surfaces typically react with surface oxygen to form CO and CO₂ [27–29]. It is therefore tempting to conclude that these peaks are due to oxidation of dissociated propene; however, water can also be seen at 540 K in Fig. 6 suggesting that not all of the propene could have completely dissociated since adsorbed H readily reacts with surface oxygen on Pd at much lower temperatures [30]. Alternatively, the structure of the lower temperature desorption features could be

influenced by limitations in the oxygen diffusion rate to the surface. That is, the rate slows just above 490 K as oxygen is depleted from the surface, and then accelerates as oxygen diffuses back to the surface, allowing oxidation of the remaining propene fragments. The O₂ desorption peak just above 700 K is consistent with oxygen desorption from either a surface oxide or PdO particles. The higher temperature peaks for CO and CO₂ above 700 K could be attributed to oxidation of carbon rings formed by condensation of C atoms released by propene dissociation, as similar high temperature TPD peaks were also observed during carbon oxidation on Pd [31–33]. The oxygen may come from chemisorbed oxygen which does not desorb from Pd (100) until over 800 K.

4. Discussion

The TPD results showed that the activation energy for CO₂ formation from propene on bulk PdO is intermediate between that seen for the surface oxide and chemisorbed oxygen. In addition, water and CO₂ desorbed simultaneously from bulk PdO, indicating a direct oxidation mechanism in which adsorbed propene, or a nearly intact fragment, is oxidized to CO₂ and water. This mechanism is similar to the surface oxide, but different from metallic Pd surfaces covered with chemisorbed oxygen where propene dissociates and then the fragments oxidize [7]. The TPD and isothermal oxygen titration experiments both revealed propene sticking coefficients close to one on the bulk oxide, or a factor of 20 higher than on the surface oxide. Together, these results indicate that the oxide is more reactive for hydrocarbon oxidation than the metal because of the lower activation energy direct pathway, and more reactive than the surface oxide because of the high sticking coefficient. The results raise several key questions, including: why is the mechanism different on the metal than on the surface and bulk oxides? Why is the activation energy higher on the bulk oxide than on the surface oxide? Why is the sticking coefficient much higher on the bulk oxide than on the surface oxide?

The differences between the reactivity of the surface oxygen phases cannot be entirely related to differences in how strongly oxygen is bound to the surfaces. We recently showed that there is little difference in oxygen desorption kinetics between the surface and bulk oxides, despite a 0.3 eV difference in the Pd 3d_{5/2} XPS peak position [34], suggesting that the oxygen bonding strengths are similar [14]. Although desorption of chemisorbed oxygen peaks roughly 100 K higher than oxygen from PdO, the stronger bonding does not explain why the reaction mechanism is different on the chemisorbed oxygen-covered metal surface. Previous propene TPD experiments showed that water desorbs from the chemisorbed oxygen-covered surface at 430 K [7], the same temperature as the surface oxide. Since at these temperatures adsorbed hydrogen and oxygen atoms on Pd rapidly react to form water which promptly desorbs [24], this indicates that the barrier to breaking C–H bonds on the surface oxide and the chemisorbed oxygen-covered surface are similar. The desorption of CO₂ at 550 K from the chemisorbed oxygen-covered Pd surface, however, indicates a higher barrier to either forming C–O bonds or break-

ing C–C bonds on the metallic surface. Because oxygen tends to island at low coverages on Pd surfaces, and because it can be compressed from a low coverage $p(2 \times 2)$ phase to higher coverage $c(2 \times 2)$ and reconstructed phases on Pd(100) [13,15,16], after the water desorbs from the chemisorbed oxygen-covered surface there is space available for the remaining C atoms to bond to the metal surface. Carbon interacts strongly with Pd and thus the higher activation energy for CO₂ formation on the chemisorbed oxygen-covered surface can reflect deeper adsorption wells for both C and O.

The much higher sticking coefficient and somewhat higher reaction temperature for the bulk oxide compared to the surface oxide cannot be readily explained with the data at hand. As noted in Section 1, low energy ion scattering indicates that the surface and bulk oxides expose similar surface densities of Pd atoms [14], and so the lower sticking coefficient on the surface oxide cannot be due to an inaccessibility of Pd sites to propene on the surface oxide. As described above, oxygen bonding strengths appear to be similar on the bulk and surface oxides and so this cannot explain the higher reaction temperature on the bulk oxide. Instead, structural effects may play an important role in determining the reactivity. Although hydrocarbon oxidation over Pd catalysts is considered structure insensitive, this reflects the fact that the structure of the oxide formed when metallic Pd is oxidized is insensitive to the structure of the starting surface [18]. In contrast, the surface oxide on Pd(100) has been assigned to a ruffled PdO(101) plane while the bulk oxide is in the form of poorly ordered clusters predominantly in an (001) orientation [17,34]. For PdO, the (101) orientation is non-polar and so this surface may be expected to be unreactive compared to polar (001) surfaces with a high density of defect sites. We are currently investigating the structure sensitivity of PdO-catalyzed reactions using ordered, epitaxial PdO thin films.

5. Summary

The reactivity of PdO clusters towards reduction by hydrocarbons was characterized using TPD and isothermal oxygen titration experiments, and compared with previous results for lower oxygen coverage phases on Pd. The PdO clusters were created by exposing Pd(100) to an oxygen plasma in UHV. Similar to the surface oxide, CO₂ and water produced by propene oxidation desorbed simultaneously, indicating a direct oxidation mechanism in which CO₂ is produced by oxidation of nearly-intact adsorbed propene. This is very different from chemisorbed oxygen-covered Pd surfaces where the dominant oxidation pathway is a two step process involving fragmentation followed by oxidation; oxidation of the surface C requires higher temperatures to produce CO₂ than the direct mechanism. Although the propene oxidation mechanism was similar on the surface and bulk oxides, there were a couple of important differences between the two. First, the CO₂ and water TPD peak temperatures were 60 K higher on the bulk oxide suggesting a higher activation energy for the reaction on the bulk oxide clusters. On the other hand, the propene sticking coefficient on the oxide clusters was close to one, a factor of 20 higher

than the surface oxide. As a result of the high sticking coefficient, CO₂ production peaked immediately upon exposing the oxide clusters to propene in oxygen titration experiments, as opposed to the surface oxide which requires reduction before substantial reactivity is seen. Thus, for higher temperatures, above roughly the 490 K CO₂ and water desorption peaks, the oxide clusters are more reactive for hydrocarbon oxidation than the surface oxide because of the higher sticking coefficient and more reactive than chemisorbed oxygen on metallic Pd because of the lower activation energy of the direct oxidation pathway.

Acknowledgments

The authors thank Dr. Min Li for his help in carrying out this work. This project was supported by the Petroleum Research Fund of the American Chemical Society through Grant number 42178-AC5. The authors also acknowledge the use of Yale Materials Research Science and Engineering Center facilities through NSF Grant No. DMR-0520495.

References

- [1] H. Over, Y.D. Kim, A.P. Seitsonen, S. Wendt, E. Lundgren, M. Schmid, P. Varga, A. Morgante, G. Ertl, *Science* 287 (2000) 1474.
- [2] H. Over, *Appl. Phys. A* 75 (2002) 37.
- [3] S. Wendt, A.P. Seitsonen, H. Over, *Catal. Today* 85 (2003) 167.
- [4] K. Reuter, M. Scheffler, *Phys. Rev. B* 65 (2001) 035406.
- [5] D.W. Goodman, C.H.F. Peden, M.S. Chen, *Surf. Sci.* 601 (2007) L124.
- [6] G. Zheng, E.I. Altman, *J. Phys. Chem. B* (2002) 8211.
- [7] E.I. Altman, *Surf. Sci.* 547 (2003) 108.
- [8] M. Valden, J. Pere, M. Hirismäki, S. Suhonen, M. Pessa, *Surf. Sci.* 377 (1997) 605.
- [9] M. Valden, J. Pere, N. Xiang, M. Pessa, *Chem. Phys. Lett.* 257 (1996) 289.
- [10] D. Ciuparu, M.R. Lyubovsky, E.I. Altman, L.D. Pfefferle, A. Datye, *Catal. Rev.* 44 (2002) 593.
- [11] J. Han, D. Zemlyanov, F.H. Ribeiro, *Catal. Today* 117 (2006) 506.
- [12] G. Zheng, E.I. Altman, *Surf. Sci.* 462 (2000) 151.
- [13] G. Zheng, E.I. Altman, *Surf. Sci.* 504 (2002) 253.
- [14] J. Wang, Y. Yun, E.I. Altman, *Surf. Sci.* 601 (2007) 3497.
- [15] S.-L. Chang, P.A. Thiel, *J. Chem. Phys.* 88 (1988) 2071.
- [16] S.-L. Chang, P.A. Thiel, J.W. Evans, *Surf. Sci.* 205 (1988) 117.
- [17] M. Todorova, E. Lundgren, V. Blum, et al., *Surf. Sci.* 541 (2003) 101.
- [18] J. Han, D. Zemlyanov, F.H. Ribeiro, *Surf. Sci.* 600 (2006) 2730.
- [19] J. Han, D. Zemlyanov, F.H. Ribeiro, *Surf. Sci.* 600 (2006) 2752.
- [20] T. Schalow, B. Brandt, M. Laurin, S. Schauermaier, J. Libuda, H.-J. Freund, *J. Catal.* (2006).
- [21] G. Zheng, E.I. Altman, *J. Phys. Chem. B* 106 (2002) 1048.
- [22] H. Gabasch, A. Knop-Gericke, R. Schloegl, et al., *Phys. Chem. Chem. Phys.* 9 (2007) S533.
- [23] X.C. Guo, R.J. Madix, *Catal. Lett.* 39 (1996) 1.
- [24] E.M. Stuve, S.W. Jorgensen, R.J. Madix, *Surf. Sci.* 146 (1984) 179.
- [25] S.-H. Oh, G.B. Hoflund, *J. Catal.* 245 (2007) 35.
- [26] E.I. Altman, R.E. Tanner, *Catal. Today* 85 (2003) 10.
- [27] X.C. Guo, R.J. Madix, *J. Am. Chem. Soc.* 117 (1995) 5523.
- [28] X.C. Guo, R.J. Madix, *Surf. Sci.* 391 (1997) L1165.
- [29] T. Mitsui, M.K. Rose, E. Fomin, D.F. Ogletree, M. Salmeron, *Surf. Sci.* 511 (2002) 259.
- [30] D.J. Suh, T.J. Park, S.K. Ihm, *Carbon* 31 (1993) 427.

- [31] A.L.D. Ramos, P.S. Alves, D.A.G. Aranda, M. Schmal, *Appl. Cat. A* 277 (2001) 71.
- [32] J.L. Figueiredo, M.F.R. Pereira, M.M.A. Freitas, J.J.M. Orfao, *Carbon* 37 (1999) 1379.
- [33] T. Mitsui, M.K. Rose, E. Fomin, D.F. Ogletree, M. Salmeron, *J. Chem. Phys.* 117 (2002) 5855.
- [34] S. Penner, D. Wang, B. Jenewein, H. Gabasch, B. Klotzer, A. Knop-Gericke, R. Schlögl, K. Hayek, *J. Chem. Phys.* 125 (2006) 094703.